Inorg. Chem. **2006**, *45*, 4035–4046

Increasing Structure Dimensionality of Copper(I) Complexes by Varying the Flexible Thioether Ligand Geometry and Counteranions

Rong Peng,[†] Dan Li,*[,†] Tao Wu,[†] Xiao-Ping Zhou,[†] and Seik Weng Ng[‡]

Department of Chemistry, Shantou University, Shantou, Guangdong 515063, P. R. China, and Department of Chemistry, University of Malaya, 50603 Kuala Lumpur, Malaysia

Received January 15, 2006

This work focuses on the systematic investigation of the influences of pyrimidine-based thioether ligand geometries and counteranions on the overall molecular architectures. A N-containing heterocyclic dithioether ligand 2,6-bis-(2-pyrimidinesulfanylmethyl)pyridine (**L1**) and three structurally related isomeric bis(2-pyrimidinesulfanylmethyl)-benzene (**L2**–**L4**) ligands have been prepared. On the basis of the self-assembly of CuX (X = I, Br, Cl, SCN, or CN) and the four structurally related flexible dithioether ligands, we have synthesized and characterized 10 new metal–organic entities, $Cu_4(\mathbf{L1})_2I_4$ **1**, $Cu_4(\mathbf{L1})_2Br_4$ **2**, $[Cu_2(\mathbf{L2})_2I_2 \cdot CH_3CN]_n$ **3**, $[Cu(\mathbf{L3})I]_n$ **4**, $[Cu(\mathbf{L3})Br]_n$ **5**, $[Cu(\mathbf{L3})CN]_n$ **6**, $[Cu(\mathbf{L4})CN]_n$ **7**, $[Cu_2(\mathbf{L4})I_2]_n$ **8**, $[Cu_2(\mathbf{L4})(SCN)_2]_n$ **9**, and $\{[Cu_6I_5(\mathbf{L4})_3](BF_4) \cdot H_2O\}_n$ **10**, by elemental analyses, IR spectroscopy, and X-ray crystallography. Single-crystal X-ray analyses show that the 10 Cu(I) complexes possess an increasing dimensionality from 0D (**1** and **2**) to 1D (**3**–**5**) to 2D (**6**–**9**) to 3D (**10**), which indicates that the ligand geometry takes an essential role in the framework formation of the Cu(I) complexes. The influence of counteranions and π–π weak interactions on the formation and dimensionality of these coordination polymers has also been explored. In addition, the photoluminescence properties of Cu(I) coordination polymers **4**–**10** in the solid state have been studied.

Introduction

Metallosupramolecular chemistry described by the spontaneous self-assembly of precursor metal ions and organic ligands has been a rapidly developing research area in the past decade.[1,2] Interest in the area is justified by a rich diversity of structural motifs, ranging from simple zero-dimensional oligomers to three-dimensional matrixes,[3] and numerous potential applications, such as catalysis, sorption, photochemistry, and magnetism.[4] One sophisticated tactic employed in the design of structural motifs is to combine the metal ions and organic ligands that have been encoded with the information necessary to predetermine the overall structure of the resulting product. The design of organic ligands is crucial in the construction of specific metallo-supramolecular architectures, because of the organic units that serve to connect the metallic centers and propagate the structural information expressed in metal coordination preferences throughout the extended structure. Therefore, once

* To whom correspondence should be addressed. E-mail: dli@stu.edu.cn.
[†] Shantou University.
[‡] University of Malaya.

(1) See for examples: (a) Leininger, S.; Olenyuk, B.; Stang, P. J. *Chem. Rev.* **2000**, *100*, 853. (b) Swiegers, G. F.; Malefetse, T. J. *Chem. Rev.* **2000**, *100*, 3483. (c) Moulton, B.; Zaworotko, M. J. *Chem. Rev.* **2001**, *101*, 1629. (d) Nishikiori, S.-I.; Yoshikawa, H.; Sano, Y.; Iwamoto, T. *Acc. Chem. Res.* **2005**, *38*, 227. (e) Holliday, B. J.; Mirkin, C. A. *Angew. Chem., Int. Ed.* **2001**, *40*, 2022. (f) James, S. L. *Chem. Soc. Rev.* **2003**, *32*, 276.

(2) (a) Yaghi, O. M.; Li, G.; Li, H. *Nature* **1995**, *378*, 703. (b) Yaghi, O. M.; Li, H. *J. Am. Chem. Soc.* **1995**, *117*, 10401. (c) Fujita, M.; Oguro, D.; Miyazawa, M.; Oka, H.; Yamaguchi, K.; Ogura, K. *Nature* **1995**, *378*, 469. (d) Hagrman, P. J.; Hagrman, D.; Zubieta, J. *Angew. Chem., Int. Ed.* **1999**, *38*, 2638. (e) Blake, A. J.; Champness, N. R.; Hubberstey, P.; Li, W.-S.; Withersby, M. A.; Schröder, M. *Coord. Chem. Rev.* **1999**, *183*, 117. (f) Barboiu, M.; Petit, E.; Vaughan, G. *Chem.—Eur. J.* **2004**, *10*, 2263. (g) Barboiu, M.; Vaughan, G.; Graff, R.; Lehn, J.-M. *J. Am. Chem. Soc.* **2003**, *125*, 10257.

(3) See for examples: (a) Ruben, M.; Rojo, J.; Romero-Salguero, F. J.; Uppadine, L. H.; Lehn, J.-M. *Angew. Chem., Int. Ed.* **2004**, *43*, 3644. (b) Papaefstathiou, G. S.; Friščić, T.; MacGillivray, L. R. *J. Am. Chem. Soc.* **2005**, *127*, 14160. (c) Liu, Y.; Kravtsov, V. C.; Beauchamp, D. A.; Eubank, J. F.; Eddaoudi, M. *J. Am. Chem. Soc.* **2005**, *127*, 7266. (d) Wang, X.-L.; Qin, C.; Wang, E.-B.; Li, Y.-G.; Su, Z.-M. *Chem. Commun.* **2005**, 5450. (e) Barnett, S. A.; Champness, N. R. *Coord. Chem. Rev.* **2003**, *246*, 145.

(4) (a) Seo, J. S.; Whang, D.; Lee, H.; Jun, S. I.; Oh, J.; Jeon, Y. J.; Kim, K. *Nature* **2000**, *404*, 982. (b) Dybtsev, D. N.; Chun, H.; Yoon, S. H.; Kim, D.; Kim, K. *J. Am. Chem. Soc.* **2004**, *126*, 32. (c) Choudhury, A.; Natarajan, S.; Rao, C. N. R. *Chem. Mater.* **1999**, *11*, 2316. (d) Ogawa, M.; Kuroda, K. *Chem. Rev.* **1995**, *95*, 399. (e) Zeng, M.-H.; Zhang, W.-X.; Sun, X.-Z.; Chen, X.-M. *Angew. Chem., Int. Ed.* **2005**, *44*, 3079. (f) Sra, A. K.; Andruh, M.; Kahn, O.; Golhen, S.; Ouahab, L.; Yakhmi, J. V. *Angew. Chem., Int. Ed.* **1999**, *38*, 2606. (g) Guo, F.; Sun, W. *Inorg. Chem.* **2005**, *44*, 4055. (h) Chakraborty, S.; Wadas, T. J.; Hester, H.; Flaschenreim, C.; Schmehl, R.; Eisenberg, R. *Inorg. Chem.* **2005**, *44*, 6284.

10.1021/ic060074x CCC: $33.50
Published on Web 04/22/2006

Chart 1

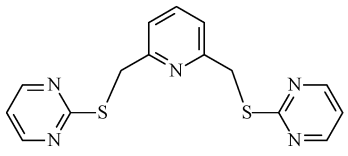

L1

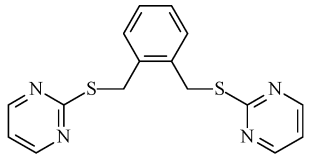

L2

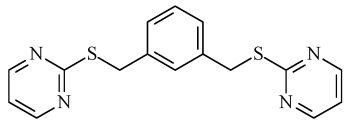

L3

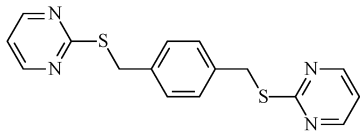

L4

suitable metal ions are recognized, variation in the geometry, size, and relative orientation of the donor groups of the organic linker can afford a tremendous breadth of structural motifs.

Taking into account the choice of organic ligands, researchers have shown thioether ligands containing a flexible backbone to be among the most important types of organic ligands, because their flexibility and conformational freedom allow for greater structural diversity. Heterocyclic-based thioether ligands bearing S- and N-coordinating sites may incline to coordinate metals with different modes, forming a great variety of structurally interesting supramolecular entities. For group 11 metals, a number of unusual and interesting supramolecular Ag(I) arrays have already been generated,[5] but Cu(I) complexes with flexible heterocyclic thioethers are less common.[6]

With regard to the metal center, the Cu(I) ion is a particularly well-suited cation not only because of its labile coordination modes with coordination numbers 2−5 but also because the associated counteranion X (X = I, Br, Cl, SCN, or CN) can be incorporated as an essential element of the framework; this offers the possibility for constructing various nuclearities and great structural complexity.

As an extension of our study of the d^{10} metal complexes with tailored properties and functions,[7] we have embarked on a program aimed at using flexible thioethers to prepare Cu(I) coordination polymers. In the course of our work, we have recently communicated a chiral 3D copper(I) coordination polymer, $\{[Cu_6I_5(\mathbf{L4})_3](BF_4)\cdot H_2O\}_n$ **10**, containing a 2D inorganic $[(Cu_6I_5)^+]_n$ layer composed of three different-directioned intersecting 1D $[CuI]_n$ helices and connected by ligand **L4** through nitrogen and sulfur atoms (**L4** = 1,4-bis(2-pyrimidinesulfanylmethyl)benzene, Chart 1).[8] To further probe the influence of systematic variations of ligand structure and counteranions on the overall molecular architectures, we prepared a series of N-containing heterocyclic thioether ligands, 2,6-bis(2-pyrimidinesulfanylmethyl)pyridine (**L1**) and three structurally related isomeric thioether ligands, bis(2-pyrimidinesulfanylmethyl)benzene (**L2**−**L4**) (Chart 1). In this contribution, 10 Cu(I) complexes of these ligands, $Cu_4(\mathbf{L1})_2I_4$ **1**, $Cu_4(\mathbf{L1})_2Br_4$ **2**, $[Cu_2(\mathbf{L2})_2I_2\cdot CH_3CN]_n$ **3**, $[Cu(\mathbf{L3})I]_n$ **4**, $[Cu(\mathbf{L3})Br]_n$ **5**, $[Cu(\mathbf{L3})CN]_n$ **6**, $[Cu(\mathbf{L4})CN]_n$ **7**, $[Cu_2(\mathbf{L4})I_2]_n$ **8**, $[Cu_2(\mathbf{L4})(SCN)_2]_n$ **9**, and $\{[Cu_6I_5(\mathbf{L4})_3](BF_4)\cdot H_2O\}_n$ **10**, have been synthesized and characterized. The series of coordination complexes (**1**−**10**) show an increasing dimensionality from 0D to 3D and allow us to have a possibility of systematically probing the effects of modifying the ligand backbone and alternating counteranions and attempting to control the precise topography (or microarchitecture) of the arrays.

Experimental Section

General. The chemicals in this work were used as purchased without further purification. Infrared spectra were obtained in KBr disks on a Nicolet Avatar 360 FTIR spectrometer in the range 4000−400 cm^{-1}. Photoluminescence analyses were performed on a Perkin−Elmer LS 55 luminescence spectrometer. Elemental analyses of C, H, and N were determined with a Perkin−Elmer 2400C elemental analyzer.

Preparation of Ligands. 2,6-Bis(2-pyrimidinesulfanylmethyl)-pyridine, L1. 2,6-Bis(bromomethyl)pyridine (2.65 g, 10 mmol) was added to a mixture of pyrimidine-2-thiolate (2.24 g, 20 mmol) and

(5) (a) Han, L.; Wu, B.; Xu, Y.; Wu, M.; Gong, Y.; Lou, B.; Chen, B.; Hong, M. *Inorg. Chim. Acta* **2005**, *358*, 2005. (b) Hong, M.; Zhao, Y.; Su, W.; Cao, R.; Fujita, M.; Zhou, Z.; Chan, A. S. C. *Angew. Chem., Int. Ed.* **2000**, *39*, 2468. (c) Hong, M.; Su, W.; Cao, R.; Fujita, M.; Lu, J. *Chem.—Eur. J.* **2000**, *6*, 427. (d) Li, K.; Xu, Z.; Fettinger, J. C. *Inorg. Chem.* **2004**, *43*, 8018. (e) Caradoc-Davies, P. L.; Hanton, L. R.; Lee, K. *Chem. Commun.* **2000**, 783. (f) Chen, C.-L.; Su, C.-Y.; Cai, Y.-P.; Zhang, H.-X.; Xu, A.-W.; Kang, B.-S. *New J. Chem.* **2003**, *27*, 790. (g) Caradoc-Davies, P. L.; Hanton, L. R. *Chem. Commun.* **2001**, 1098. (h) Amoore, J. J. M.; Black, C. A.; Hanton, L. R.; Spicer, M. D. *Cryst. Growth. Des.* **2005**, *5*, 1255. (i) Bu, X.-H.; Chen, W.; Du, M.; Biradha, K.; Wang, W.-Z.; Zhang, R.-H. *Inorg. Chem.* **2002**, *41*, 437. (j) Bu, X.-H.; Xie, Y.-B.; Li, J.-R. Zhang, R.-H. *Inorg. Chem.* **2003**, *42*, 7422. (k) Hartshorn, C. M.; Steel, P. J. *J. Chem. Soc., Dalton Trans.* **1998**, 3935.

(6) (a) Amoore, J. J. M.; Hanton, L. R.; Spicer, M. D. *Dalton Trans.* **2003**, 1056. (b) Song, R.-F.; Xie, Y.-B.; Li, J.-R.; Bu, X.-H. *CrystEngComm.* **2005**, *7*, 249. (c) Caradoc-Davies, P. L.; Hanton, L. R.; Hodgkiss, J. M.; Spicer, M. D. *J. Chem. Soc., Dalton Trans.* **2002**, 1581. (d) Park, K.-M.; Yoon, I.; Seo, J.; Lee, J.-E.; Kim, J.; Choi, K. S.; Jung, O.-S.; Lee, S. S. *Cryst. Growth. Des.* **2005**, *5*, 1707.

(7) (a) Li, D.; Wu, T.; Zhou, X.-P.; Zhou, R.; Huang, X.-C. *Angew. Chem., Int. Ed.* **2005**, *44*, 4175. (b) Li, D.; Shi, W.-J.; Hou, L. *Inorg. Chem.* **2005**, *44*, 3907. (c) Li, D.; Wu, T. *Inorg. Chem.* **2005**, *44*, 1175. (d) Wu, T.; Li, D.; Alg, S. W. *CrystEngComm.* **2005**, *7*, 514. (e) Hou, L.; Li, D.; Shi, W.-J.; Yin, Y.-G.; Ng, S. W. *Inorg. Chem.* **2005**, *44*, 7825. (f) Wu, T.; Zhou, R.; Li, D. *Inorg. Chem. Commun.* **2006**, *9*, 341.

(8) Peng, R.; Wu, T.; Li, D. *CrystEngComm* **2005**, *7*, 595.

(9) *SMART, version 5.060*; Bruker Analytical X-ray Systems: Madison, WI: 1997−1999.

(10) *SAINT, version V5.6*; Bruker Analytical X-ray Systems: Madison, WI.

CH_3ONa (1.19 g, 22 mmol) in ethanol (50 mL) under stirring. The mixture was heated to 70 °C for 8 h with vigorous stirring. It was then filtered and concentrated to give **L1** as a pale-yellow solid, which was washed with water and dried in air (65% yield). Mp: 95−97 °C. IR (KBr pellet, cm^{-1}): 2921m, 2847w, 1638m, 1560s, 1450m, 1380s, 1168m, 1053s, 747w, 628w. Anal. Calcd for $C_{15}H_{14}N_5S_2$: C, 55.02; H, 4.00; N, 21.39. Found: C, 55.10; H, 4.05; N, 21.28. Single crystals suitable for X-ray crystallography were grown by slow diffusion of diethyl ether into an acetonitrile solution of **L1**.

1,2-Bis(2-pyrimidinesulfanylmethyl)benzene, L2. 1,2-Bis(bromomethyl)benzene (2.64 g, 10 mmol) was added to a mixture of pyrimidine-2-thiolate (2.24 g, 20 mmol) and CH_3ONa (1.19 g, 22 mmol) in ethanol (50 mL) with stirring. The mixture was heated to 60 °C for 6 h with vigorous stirring. It was then filtered and concentrated to give **L2** as a yellow oil, which afforded a light yellow powder by recrystallization from CH_2Cl_2/Et_2O/hexane. (70% yield). Mp: 62−64 °C. IR (KBr pellet, cm^{-1}): 3109w, 3052w, 2921m, 2848w, 1650m, 1552s, 1458w, 1380s, 1172s, 1078m, 800w, 767m. Anal. Calcd for $C_{16}H_{14}N_4S_2$: C, 58.87; H, 4.32; N, 17.16. Found: C, 58.89; H, 4.26; N, 17.12.

1, 3-Bis(2-pyrimidinesulfanylmethyl)benzene, L3. Reaction of 1,3-bis(bromomethyl)benzene (2.64 g, 10 mmol) with pyrimidine-2-thiolate (2.24 g, 20 mmol) and CH_3ONa (1.19 g, 22 mmol) as described above for **L1** gave ligand **L3** as a pale-yellow solid (80% yield). Mp: 67−69 °C. IR (KBr pellet, cm^{-1}): 3037w, 2922m, 2853w, 1638w, 1556s, 1376s, 1172m, 1061m, 795w, 709w. Anal. Calcd for $C_{16}H_{14}N_4S_2$: C, 58.87; H, 4.32; N, 17.16. Found: C, 58.99; H, 4.12; N, 17.29. Single crystals suitable for X-ray crystallography were grown by slow diffusion of diethyl ether into a dichloromethane solution of **L3**.

1,4-Bis(2-pyrimidinesulfanylmethyl)benzene, L4. Reaction of 1,4-bis(bromomethyl)benzene (2.64 g, 10 mmol) with pyrimidine-2-thiolate (2.24 g, 20 mmol) and CH_3ONa (1.19 g, 22 mmol) as described above for **L1** gave **L4** as a colorless needle crystal (90% yield). Mp: 154−156 °C. IR (KBr pellet, cm^{-1}): 2970m, 2925m, 2868w, 1728s, 1650w, 1548s, 1376s, 1180m, 1111m, 1066w, 775m, 747w. Anal. Calcd for $C_{16}H_{14}N_4S_2$: C, 58.87; H, 4.32; N, 17.16. Found: C, 58.69; H, 4.39; N, 17.22. Single crystals suitable for X-ray crystallography were grown by slow diffusion of diethyl ether into a dichloromethane solution of **L4**.

Preparation of Cu(I) Complexes. $Cu_4(L1)_2I_4$, 1. A solution of CuI (0.038 g, 0.2 mmol) in acetonitrile (4 mL) was added to a solution of **L1** (0.032 g, 0.1 mmol) in DMF (2 mL). The reaction mixture was stirred for 30 min to give a yellow solution. Slow diffusion of diethyl ether into the filtrate yielded yellow block crystals of **1** in two weeks (24% yield). IR (KBr pellet, cm^{-1}): 2917w, 2880w, 1973w, 1589w, 1552s, 1450m, 1373s, 1184s, 812w, 759m, 637w. Anal. Calcd for $C_{30}H_{26}Cu_4I_4N_{10}S_4$: C, 25.43; H, 1.85; N, 9.89. Found: C, 25.62; H, 1.74; N, 9.72.

$Cu_4(L1)_2Br_4$, 2. The reaction of CuBr (0.029 g, 0.2 mmol) and **L1** (0.032 g, 0.1 mmol) as described above for **1** gave yellow block crystals of **2** (18% yield). IR (KBr pellet, cm^{-1}): 2921m, 2843w, 1744w, 1646m, 1556s, 1454m, 1373s, 1176s, 808w, 751m. Anal. Calcd for $C_{30}H_{26}Cu_4Br_4N_{10}S_4$: C, 29.33; H, 2.13; N, 11.40. Found: C, 29.15; H, 2.25; N, 11.24.

$[Cu_2(L2)_2I_2 \cdot CH_3CN]_n$, 3. A solution of CuI (0.019 g, 0.1 mmol) in a KI-saturated solution (2 mL) was added to a solution of **L2** (0.032 g, 0.1 mmol) in acetonitrile (4 mL). The reaction mixture was stirred for 30 min to give a yellow solution that was then filtered. Yellow block crystals of **3** were formed by slow evaporation after three weeks (40% yield). IR (KBr pellet, cm^{-1}): 2921w, 2848w, 1634m, 1565s, 1544s, 1381s, 1180s, 1074m, 800w, 764m. Anal. Calcd for $C_{34}H_{31}Cu_2I_2N_9S_4$: C, 38.00; H, 2.91; N, 11.73. Found: C, 37.78; H, 3.03; N, 11.77.

$[Cu(L3)I]_n$, 4. A mixture of CuI (0.019 g, 0.1 mmol), **L3** (0.032 g, 0.1 mmol), a KI-saturated solution (2.0 mL), and acetonitrile (4.0 mL) was stirred for 15 min. It was then transferred and sealed in a 13 mL Teflon-lined stainless steel reactor, which was heated in an oven to 120 °C for 48 h and then cooled to room temperature at a rate of 3 °C 0.5 h^{-1}. The reaction mixture was filtered to give a yellow solution. Yellow crystals of **4** were obtained by slow evaporation in two weeks (38% yield). IR (KBr pellet, cm^{-1}): 3048m, 2921m, 2848w, 1646w, 1552s, 1475w, 1377s, 1184s, 1074m, 804m, 755m. Anal. Calcd for $C_{16}H_{14}CuIN_4S_2$: C, 37.18; H, 2.73; N, 10.84. Found: C, 37.21; H, 2.59; N, 10.70.

$[Cu(L3)Br]_n$, 5. A mixture of CuBr (0.014 g, 0.1 mmol), **L3** (0.032 g, 0.1 mmol), and acetonitrile (6.0 mL) was stirred for 15 min. It was then transferred and sealed in a 13 mL Teflon-lined stainless steel reactor, which was heated in an oven to 120 °C for 48 h and then cooled to room temperature at a rate of 3 °C 0.5 h^{-1}. Yellow block crystals of **5** were attained (27% yield). IR (KBr pellet, cm^{-1}): 3044w, 2921w, 2848w, 1617m, 1548s, 1426m, 1381s, 1185s, 1037m, 800w, 760w. Anal. Calcd for $C_{16}H_{14}CuBrN_4S_2$: C, 40.90; H, 3.00; N, 11.92. Found: C, 40.82; H, 2.85; N, 12.01.

$[Cu(L3)CN]_n$, 6. A mixture of CuCN (0.009 g, 0.1 mmol), **L3** (0.032 g, 0.1 mmol), benzene (2.0 mL), and acetonitrile (4.0 mL) was stirred for 15 min. It was then transferred and sealed in a 13 mL Teflon-lined stainless steel reactor, which was heated in an oven to 120 °C for 48 h and then cooled to room temperature at a rate of 3 °C 0.5 h^{-1}. The reaction mixture was filtered to give a pale-yellow solution. Pale-yellow plate crystals of **6** were attained by slow evaporation in two weeks (20% yield). IR (KBr pellet, cm^{-1}): 2921w, 2847w, 2128m, 1642m, 1552s, 1380s, 1196w, 1168w, 1053m, 800w, 710w. Anal. Calcd for $C_{17}H_{14}CuN_5S_2$: C, 49.08; H, 3.39; N, 16.84. Found: C, 49.20; H, 3.25; N, 16.77.

$[Cu(L4)CN]_n$, 7. A mixture of CuCN (0.009 g, 0.1 mmol), **L4** (0.032 g, 0.1 mmol), benzene (2.0 mL), and acetonitrile (4.0 mL) was stirred for 15 min. It was then transferred and sealed in a 13 mL Teflon-lined stainless steel reactor, which was heated in an oven to 140 °C for 48 h and then cooled to room temperature at a rate of 3 °C 0.5 h^{-1}. Pale-yellow block crystals of **7** were attained (54% yield). IR (KBr pellet, cm^{-1}): 2917m, 2848w, 2132m, 1728w, 1642m, 1552s, 1377s, 1160w, 1054s, 763w. Anal. Calcd for $C_{17}H_{14}CuN_5S_2$: C, 49.04; H, 3.37; N, 16.84. Found: C, 49.14; H, 3.30; N, 16.75.

Other methods: The procedure was the same as above using CuI/CuBr/CuCl instead of CuCN in the presence of CH_3CN and other auxiliary solvents such as DMF, benzene, toluene, ethanol, isopropyl alcohol, etc. Pale-yellow block crystals of **7** were obtained directly or indirectly by growing them from mother liquors in a month (15−38% yield).

$[Cu_2(L4)I_2]_n$, 8. A mixture of CuI (0.038 g, 0.2 mmol), **L4** (0.032 g, 0.1 mmol), hexane (2.0 mL), and acetonitrile (4.0 mL) was stirred for 15 min. It was then transferred and sealed in a 13 mL Teflon-lined stainless steel reactor, which was heated in an oven to 120 °C for 48 h and then cooled to room temperature at a rate of 3 °C 0.5 h^{-1}. Pale-yellow plate crystals of **8** were obtained (23% yield). IR (KBr pellet, cm^{-1}): 2960m, 1730m, 1620w, 1550w, 1380s, 1180s, 1070s, 467m. Anal. Calcd for $C_8H_7CuIN_2S$: C, 27.17; H, 1.99; N, 7.92. Found: C, 27.31; H, 1.89; N, 7.88.

$[Cu_2(L4)(SCN)_2]_n$, 9. A mixture of CuSCN (0.024 g, 0.2 mmol), **L4** (0.032 g, 0.1 mmol), benzene (2.0 mL), and acetonitrile (4.0 mL) was stirred for 15 min. It was then transferred and sealed in a 13 mL Teflon-lined stainless steel reactor, which was heated in

Table 1. Summary of the Crystal Data and Structure Refinement Parameters for **L1**, **L3**, **L4**, and **1**−**10**

	L1	**L3**	**L4**	**1**	**2**	**3**
formula	$C_{30}H_{26}N_{10}S_4$	$C_{16}H_{14}N_4S_2$	$C_{16}H_{14}N_4S_2$	$C_{30}H_{26}Cu_4I_4N_{10}S_4$	$C_{30}H_{26}Cu_4Br_4N_{10}S_4$	$C_{34}H_{31}Cu_2I_2N_9S_4$
fw	654.85	326.43	326.43	1416.61	1228.65	1074.80
cryst syst	monoclinic	monoclinic	monoclinic	monoclinic	monoclinic	triclinic
space group	$P2_1$	Pc	$P2_1/a$	$P2_1/n$	$P2_1/n$	$P\bar{1}$
a (Å)	6.3410(5)	13.953(3)	12.0861(8)	13.2104(10)	13.1282(9)	11.5768(6)
b (Å)	12.2842(11)	4.6420(10)	4.6576(3)	9.9479(8)	9.7714(7)	12.7908(6)
c (Å)	20.2427(18)	12.389(3)	27.9405(18)	15.2018(11)	14.8445(10)	15.2079(7)
α (deg)	90	90	90	90	90	99.393(1)
β (deg)	90.296(2)	103.550(4)	102.513(1)	95.757(1)	95.552(1)	101.457(1)
γ (deg)	90	90	90	90	90	109.878(1)
V (Å^3)	1576.8(2)	780.1(3)	1535.47(17)	1987.7(3)	1895.3(2)	2009.46(17)
Z	2	2	4	2	2	2
T (K)	293(2)	293(2)	293(2)	293(2)	293(2)	293(2)
D_{calcd} (g cm^{-3})	1.379	1.390	1.412	2.367	2.153	1.776
μ (mm^{-1})	0.341	0.342	0.348	5.466	6.691	2.840
no. of reflns collected	10096	3790	12987	12262	11721	17397
no. of unique reflns	5209	1925	3466	4601	4412	8989
R_{int}	0.0419	0.0238	0.0255	0.0270	0.0259	0.0159
R1 [$I > 2\sigma(I)$]	0.0802	0.0562	0.0478	0.0414	0.0406	0.0304
wR2 [$I > 2\sigma(I)$]	0.1663	0.1417	0.1168	0.0935	0.0889	0.0793
R1 [all reflns]	0.1170	0.0601	0.0541	0.0569	0.0585	0.0364
wR2 [all reflns]	0.1860	0.1497	0.1270	0.1002	0.0956	0.0872
ρ_{fin} (max/min) (e Å^{-3})	0.848/−0.294	0.485/−0.182	0.444/−0.181	1.785/−0.921	1.514/−1.264	0.855/−0.814

	4	**5**	**6**	**7**	**8**	**9**	**10**
formula	$C_{16}H_{14}CuIN_4S_2$	$C_{16}H_{14}CuBrN_4S_2$	$C_{17}H_{14}CuN_5S_2$	$C_{17}H_{14}CuN_5S_2$	$C_8H_7CuIN_2S$	$C_{18}H_{14}Cu_2N_6S_4$	$C_{48}H_{44}BCu_6F_4I_5N_{12}OS_6$
fw	516.87	469.88	415.99	415.99	353.66	569.68	2099.86
cryst syst	monoclinic	monoclinic	orthorhombic	orthorhombic	monoclinic	monoclinic	hexagonal
space group	$C2/c$	$C2/c$	$Pnc2$	$Pca2_1$	$P2_1/c$	$C2/c$	$P6_3$
a (Å)	29.755(2)	29.830(3)	14.0560(12)	12.3143(11)	4.3816(5)	11.7761(14)	13.5662(7)
b (Å)	13.4624(9)	13.1418(11)	4.8159(4)	4.8205(4)	16.8590(19)	17.229(2)	13.5662
c (Å)	8.9729(6)	8.7840(7)	12.5757(11)	28.265(3)	13.1538(14)	10.4611(13)	20.1867(11)
α (deg)	90	90	90	90	90	90	90
β (deg)	99.333(2)	98.868(2)	90	90	93.384(2)	97.777(2)	90
γ (deg)	90	90	90	90	90	90	120
V (Å^3)	3546.7(4)	3402.4(5)	851.28(13)	1677.9(3)	969.97(19)	2102.9(5)	3217.5(2)
Z	8	8	2	4	4	4	2
T (K)	293(2)	293(2)	293(2)	293(2)	293(2)	293(2)	293(2)
D_{calcd} (g cm^{-3})	1.936	1.835	1.623	1.647	2.422	1.799	2.167
μ (mm^{-1})	3.213	3.883	1.538	1.561	5.599	2.439	4.599
no. of reflns collected	15057	10473	4773	7961	5913	6334	17484
no. of unique reflns	4135	3870	1809	2916	2223	2412	3830
R_{int}	0.0243	0.0203	0.0191	0.0323	0.0239	0.0227	0.0318
R1 [$I > 2\sigma(I)$]	0.0339	0.0281	0.0592	0.0509	0.0322	0.0392	0.0335
wR2 [$I > 2\sigma(I)$]	0.0816	0.0671	0.1883	0.1135	0.0768	0.0892	0.0915
R1 [all reflns]	0.0438	0.0351	0.0629	0.0624	0.0389	0.0495	0.0375
wR2 [all reflns]	0.0962	0.0699	0.1999	0.1198	0.0798	0.0986	0.1001
ρ_{fin} (max/min) (e Å^{-3})	0.780/−0.549	0.560/−0.366	0.421/−0.469	0.605/−0.284	1.128/−0.861	0.606/−0.326	1.283/−0.805

an oven to 140 °C for 48 h and then cooled to room temperature at a rate of 3 °C 0.5 h^{-1}. The reaction mixture was filtered to give a yellow solution. Yellow transparent crystals of **9** were obtained by slow evaporation in two weeks (11% yield). IR (KBr pellet, cm^{-1}): 2921m, 2848w, 2112m, 1638m, 1556m, 1385s, 1061s, 760w, 673w. Anal. Calcd for $C_{18}H_{14}Cu_2N_6S_4$: C, 37.95; H, 2.48; N, 14.75. Found: C, 37.80; H, 2.55; N, 14.68.

{[Cu$_6$I$_5$(L4)$_3$](BF$_4$)·H$_2$O}$_n$ 10. See our previous communication[8] for details.

Crystallography. Suitable crystals of **L1**, **L3**, **L4**, and **1**−**10** were mounted with glue at the end of a glass fiber. Data collection was performed on a Bruker Smart Apex CCD diffractometer (Mo Kα, $\lambda = 0.71073$ Å) using SMART.[9] Parameters for data collection and refinement of the three ligands and nine complexes are summarized in Table 1. Reflection intensities were integrated using SAINT software,[10] and absorption correction was applied.[11] The structures were solved by direct methods and refined by full-matrix least-squares refinements based on F^2. Anisotropic thermal parameters were applied to all non-hydrogen atoms. The hydrogen atoms were generated geometrically (C−H = 0.960 Å). The crystallographic calculations were conducted using the SHELXL-97 programs. The orientation of the bridging cyanide group in **6** and **7** was found to be disordered, and the C and N atoms were refined with a 50% probability of being C or N. In this paper, the atoms in all such groups are labeled C/N(1), etc., as a reminder of the possible disorder. Selected bond lengths and angles for complexes **1**−**10** are given in Tables 2−4.

(11) Sheldrick, G. M. *SADABS*; University of Göttingen: Göttingen, Germany, 1996 and 2003.

Table 2. Selected Bond Lengths (Å) and Bond Angles (deg) for Complexes **1**−**3**[a]

		Complex **1**	
Cu(1)−I(2)	2.5777(9)	N(3)−Cu(1)−I(2)	127.94(12)
Cu(1)−N(3)	2.077(4)	N(3)−Cu(1)−I(1)	119.97(12)
Cu(1)−S(2)	2.6200(17)	I(2)−Cu(1)−I(1)	111.75(3)
Cu(1)−S(1)	2.7380(17)	S(2)−Cu(1)−S(1)	160.01(5)
Cu(1)−Cu(2)	2.87771(6)	N(1A)-Cu(2)−I(2)	106.24(12)
Cu(1)−I(1)	2.6510(9)	N(1A)-Cu(2)−I(1)	113.33(12)
Cu(2)−I(1)	2.6220(8)	I(2)−Cu(2)−I(1)	111.42(3)
Cu(2)−Cu(2A)	2.9649(15)	N(1A)−Cu(2)−I(1A)	105.87(12)
Cu(2)−I(1A)	2.7770(9)	I(2)−Cu(2)−I(1A)	105.95(3)
Cu(2)−N(1A)	2.069(4)	I(1)−Cu(2)−I(1A)	113.45(3)
Cu(2)−I(2)	2.6174(9)		
		Complex **2**	
Cu(1)−Cu(2)	2.8162(8)	N(3A)−Cu(1)−Br(1)	129.87(9)
Cu(1)−Br(1)	2.4448(7)	N(3A)−Cu(1)−Br(2)	120.24(9)
Cu(1)−Br(2)	2.5341(7)	Br(1)−Cu(1)−Br(2)	109.37(2)
Cu(1)−N(3A)	2.065(3)	S(1A)−Cu(1)−S(2A)	161.10(4)
Cu(1)−S(1A)	2.5855(12)	N(5)−Cu(2)−Br(2)	117.59(9)
Cu(1)−S(2A)	2.7187(12)	N(5)−Cu(2)−Br(1)	107.64(9)
Cu(2)−N(5)	2.040(3)	Br(2)−Cu(2)−Br(1)	110.54(3)
Cu(2)−Cu(2A)	2.9820(12)	N(5)−Cu(2)−Br(2A)	105.56(9)
Cu(2)−Br(2)	2.4682(7)	Br(2)−Cu(2)−Br(2A)	109.51(2)
Cu(2)−Br(2A)	2.6897(8)	Br(1)−Cu(2)−Br(2A)	105.21(3)
Cu(2)−Br(1)	2.4756(7)		
		Complex **3**	
Cu(1)−I(1)	2.6166(4)	N(4)−Cu(1)−N(7B)	119.54(9)
Cu(1)−I(2)	2.7125(5)	N(4)−Cu(1)−I(1)	112.37(7)
Cu(1)−N(4)	2.045(2)	N(7B)−Cu(1)−I(1)	106.30(6)
Cu(1)−N(7B)	2.072(2)	N(4)−Cu(1)−I(2)	106.05(7)
Cu(2)−I(1)	2.7040(4)	N(7B)−Cu(1)−I(2)	100.59(7)
Cu(2)−I(2)	2.6587(4)	I(1)−Cu(1)−I(2)	111.380(15)
Cu(2)−N(5)	2.044(2)	N(5)−Cu(2)−N(2A)	120.38(9)
Cu(2)−N(2A)	2.066(2)	N(5)−Cu(2)−I(2)	110.55(7)
Cu(2)−Cu(1)	3.0262(6)	N(2A)−Cu(2)−I(2)	106.55(7)
		N(5)−Cu(2)−I(1)	104.42(7)
		N(2A)−Cu(2)−I(1)	104.23(7)
		I(2)−Cu(2)−I(1)	110.345(14)

[a] Symmetry codes for **1**: A $-x+2, -y+2, -z$; for **2**: A $-x+2, -y+1, -z+2$; for **3**: A $x, y+1, z$; B $x, y-1, z$.

Table 3. Selected Bond Lengths (Å) and Bond Angles (deg) for Complexes **4**−**6**[a]

		Complex **4**	
Cu(1)−I(1)	2.8424(6)	N(1)−Cu(1)−N(4B)	137.02(11)
Cu(1)−N(1)	2.013(3)	N(1)−Cu(1)−I(1A)	107.65(8)
Cu(1)−N(4B)	2.013(3)	N(4B)−Cu(1)−I(1A)	105.76(8)
Cu(1)−I(1A)	2.6865(6)	N(1)−Cu(1)−I(1)	93.34(8)
		N(4B)−Cu(1)−I(1)	105.79(8)
		I(1A)−Cu(1)−I(1)	101.351(19)
		Complex **5**	
Cu(1)−N(4)	1.9891(18)	N(4)−Cu(1)−N(1B)	140.37(7)
Cu(1)−N(1B)	1.9972(17)	N(4)−Cu(1)−Br(1A)	105.69(5)
Cu(1)−Br(1A)	2.5418(4)	N(1B)−Cu(1)−Br(1A)	106.83(5)
Cu(1)−Br(1)	2.7008(4)	N(4)−Cu(1)−Br(1)	104.69(5)
		N(1B)−Cu(1)−Br(1)	93.08(5)
		Br(1A)−Cu(1)−Br(1)	97.216(14)
		Complex **6**	
Cu(1)−C/N(1)	1.885(7)	C/N(1)−Cu(1)−C/N(1A)	155.2(4)
Cu(1)−C/N(1A)	1.885(7)	C/N(1)−Cu(1)−N(1A)	93.5(2)
Cu(1)−N(1A)	2.431(6)	C/N(1A)−Cu(1)−N(1A)	103.7(3)
Cu(1)−N(1)	2.431(6)	C/N(1)−Cu(1)−N(1)	103.7(3)
		C/N(1A)−Cu(1)−N(1)	93.5(2)
		N(1A) −Cu(1)−N(1)	91.9(3)

[a] Symmetry codes for **4**: A $-x+2, y, -z+5/2$; B $x, y, z+1$; for **5**: A $-x+2, y, -z+1/2$; B $x, y, z-1$; for **6**: A $-x+1, -y, z$.

Results and Discussion

Syntheses. The three isomeric bis(2-pyrimidinesulfanylmethyl)benzene compounds (**L2**−**L4**) and the related 2,6-bis(2-pyrimidinesulfanylmethyl)pyridine (**L1**) were prepared conveniently in high yields by the reactions of pyrimidine-2-thiolate with 1,2-bis(bromomethyl)benzene, 1,3-bis(bromomethyl)benzene, 1,4-bis(bromomethyl)benzene, and 2,6-bis(bromomethyl)pyridine, respectively, in a 2:1 molar ratio under heating conditions. **L1**−**L3** are soluble in common polar organic solvents, but **L4** is less soluble except in DMF, THF, and chlorinated solvents, which does not facilitate the solution reaction between **L4** and inorganic metal salts.

Table 4. Selected Bond Lengths (Å) and Bond Angles (deg) for Complexes **7**−**10**[a]

		Complex **7**	
Cu(1)−C/N(2)	1.871(6)	C/N(2)−Cu(1)−C/N(1)	154.96(16)
Cu(1)−C/N(1)	1.889(4)	C/N(2)−Cu(1)−N(4)	103.3(3)
Cu(1)−N(4)	2.333(7)	C/N(1)−Cu(1)-N(4)	93.9(3)
Cu(1)−N(2A)	2.521(2)	C/N(2)−Cu(1)−N(2A)	97.3
		C/N(1)−Cu(1)−N(2A)	99.8
		N(2A)−Cu(1)−N(4)	93.2
		Complex **8**	
Cu(1)−I(1)	2.5602(7)	N(1)−Cu(1)−I(1)	138.75(9)
Cu(1)−I(1A)	2.6939(7)	N(1)−Cu(1)−I(1A)	101.52(9)
Cu(1)−I(1B)	3.0338(8)	I(1)−Cu(1)−I(1A)	112.99(2)
Cu(1)−N(1)	2.017(3)	N(1)−Cu(1)−I(1B)	96.92(10)
		I(1)−Cu(1)−I(1B)	92.51(2)
		I(1A)−Cu(1)−I(1B)	109.26(2)
		Complex **9**	
Cu(1)−N(1)	2.031(2)	N(1A)−Cu(1)−N(1)	144.47(12)
Cu(1)−N(1A)	2.031(2)	N(1A)−Cu(1)−S(2A)	101.26(6)
Cu(1)−S(2)	2.4756(8)	N(1)−Cu(1)−S(2A)	98.80(6)
Cu(1)−S(2A)	2.4756(8)	N(1A)−Cu(1)−S(2)	98.80(6)
Cu(2)−N(3)	1.900(2)	N(1)−Cu(1)−S(2)	101.26(6)
Cu(2)−N(3A)	1.900(2)	S(2A)−Cu(1)−S(2)	110.40(4)
Cu(2)−S(2)	2.5911(8)	N(3)−Cu(2)−N(3A)	147.71(15)
Cu(2)−S(2A)	2.5911(8)	N(3)−Cu(2)−S(2)	100.33(8)
S(2)−C(9)	1.648(3)	N(3A)−Cu(2)−S(2)	99.53(8)
N(3B)−C(9)	1.151(4)	N(3)−Cu(2)−S(2A)	99.53(8)
		N(3A)−Cu(2)−S(2A)	100.33(8)
		S(2)−Cu(2)−S(2A)	103.36(4)
		N(3B)−C(9)−S(2)	179.8(3)
		Complex **10**	
Cu(1)−I(1)	2.6821(11)	N(4E)−Cu(1)−S(2F)	116.53(18)
Cu(1A)−I(1)	2.6821(11)	N(4E)−Cu(1)−I(2)	106.61(17)
Cu(1B)−I(1)	2.6821(11)	S(2F)−Cu(1)−I(2)	106.65(6)
Cu(1)−I(2)	2.6417(11)	N(4E)−Cu(1)−I(1)	109.46(16)
Cu(2)−I(2)	2.6446(11)	S(2F)−Cu(1)−I(1)	104.07(6)
Cu(2C)−I(3)	2.6140(11)	I(2)−Cu(1)−I(1)	113.73(4)
Cu(2D)−I(3)	2.6140(11)	N(1C)−Cu(2)−S(1)	112.68(19)
Cu(2)−I(3)	2.6140(11)	N(1C)−Cu(2)−I(3)	113.87(18)
Cu(1)−N(4E)	2.049(6)	S(1)−Cu(2)−I(3)	106.01(6)
Cu(1)−S(2F)	2.334(2)	N(1C)−Cu(2)−I(2)	107.97(18)
Cu(2)−N(1C)	2.030(7)	S(1)−Cu(2)−I(2)	106.27(6)
Cu(2)−S(1)	2.360(2)	I(3)−Cu(2)−I(2)	109.76(4)

[a] Symmetry codes for **7**: A $1/2-x, y, -1/2+z$; for **8**: A $x+1, y, z$; B $-x+1, -y+2, -z+1$; for **9**: A $-x+2, y, -z+5/2$; B $-x+2, -y, -z+2$; for **10**: A $-x+y, -x, z$; B $-y, x-y, z$; C $-x+y, -x+1, z$; D $-y+1, x-y+1, z$; E $-x, -y, z+1/2$; F $y, -x+y, z+1/2$.

The complexes were synthesized with the corresponding metal:ligand ratios. Crystals of **4**−**10** were obtained directly from solvothermal conditions or grown indirectly from the resulting mother liquor of solvothermal reactions, which certainly contains richer content than the resulting solution from the conventional method. This is the first time that the hydro(solvo)thermal method was adopted in the construction of metal−organic frameworks of flexible thioether ligands. It is well-known that hydro(solvo)thermal reactions can not only enhance metal−ligand interactions but also produce

metastable compounds that may not be accessible by the conventional method, which promotes crystal growth because the nature and temperature of the hydro(solvo)thermal fluid can be varied over a wide range. The assembly of a number of rigid ligands and metal salts produced various new coordination polymeric solids with beautiful architectures and interesting topologies.[12] However, self-assembly reactions of metal ions and flexible thioether ligands always adopted a conventional solution method under ambient conditions because the cleavage reaction on C−S of thioether ligands took place easily under high temperature and pressure.[5,6] In this work, in view of the difficulty with copper(I) halides and pseudo-halides being extreme insoluble in common solvents in air, whereas they can be easily dissolved in hydro(solvo)thermal condition,[7c−d,13] we tried the solvothermal reactions of CuX (X = I, Br, Cl, SCN, or CN) and thioether ligands with a lower temperature and shorter reaction time, avoiding the C−S bond cleavage. The stability of the four thioether ligands in the order of **L4** > **L3** > **L2** > **L1** was indicated through a large number of experiments in which **L4** could exist stably up to 140 °C, whereas the cleavage on C−S of **L1** had taken place below 100 °C to form black metallic sulfide. Therefore, both the conventional solution layer diffusion and the hydrothermal methods were adopted in this work to deal with the difference in ligand stability.

Interestingly, complex **7** could be prepared under solvothermal conditions with CuCN/CuI/CuBr/CuCl, and **L4** in mixed solvents of CH_3CN and other auxiliary solvents. The C−C bond cleavage and release of cyanide for organonitriles are not surprising under solvothermal conditions.[14] Except for the direct addition of CuCN, the generation of cyanide **7** by the reactions of CuI/CuBr/CuCl might be due to the decomposition of solvent acetonitrile at the relatively high temperature (140 °C) and autogenous pressure of the reaction. Presumably, the formation of the 2D polymer $[Cu(\mathbf{L4})CN]_n$ might be because the stability of the crystal structures composed of cyanide anion is superior to that of structures composed of halogenous anion. Obviously, the stripping of cyanide ion from a CH_3CN solvent provides the source for the capping anion in the aggregation of coordination architectures.

Crystal Structures. Free ligands. Three ligands, **L1**, **L3**, and **L4**, all crystallize in a monoclinic system with two independent molecules, one independent molecule, and two crystallographically nonequivalent half-molecules in asymmetric units, respectively. As shown in Figure 1, all three ligands are twisted; their torsion angles and dihedral angles for structural comparison are summarized in Table 5. It should be noted that there is a considerable difference in the torsion angles and dihedral angles between **L1** and **L3**, although only the N atom in the pyridyl ring of **L1** is replaced by a carbon atom in the central phenyl of **L3**. It seems that the interaction of the $N_{pyridine}$ lone-pair electrons plays an important role in determining the conformation of the free ligand **L1**, placing the two pyrimidyl with the central pyridyl in a syn conformation. The **L1** molecule containing one $N_{pyridine}$ and two S as a tridentate ligand possesses the expected ability to chelate a metal atom, forming two five-membered rings (NC_2SM). In contrast, the half-spiral structure of the **L4** molecule with the two pyrimidyl groups in the anti positions of the central benzene seems to be favorable for the formation of a helical complex. Different from **L1** and **L3**, the outer pyrimidine groups in **L4** are coplanar and orient trans to each other, which conform **L4** to a *Z*-like structure.

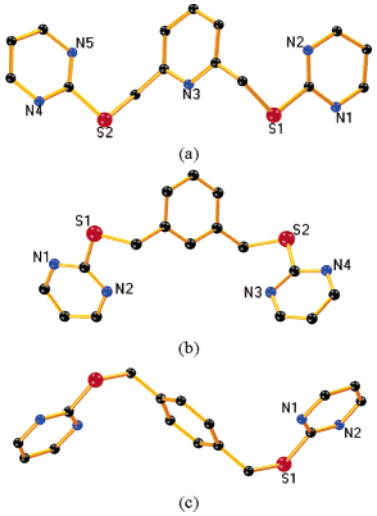

Figure 1. Basic molecules of (a) **L1**, (b) **L3**, and (c) **L4**.

Table 5. Comparison of Torsion Angles and Dihedral Angles of Free Ligands

	TA[a] (deg)	DA[b] (deg)	DA[c] (deg)
L1	−79.5(5), −84.0(5), 79.4(5), 84.5(5)	61.5−70.3	16.7−19.9
L3	92.5(5), 98.1(5)	61.1−63.1	67.4
L4	−84.0(2), 85.2(2)	66.5−68.2	0

[a] Torsion angles of $C_{(pyrimidyl)}-S-C_{(methylene)}-C_{(phenyl)}$. [b] Dihedral angles between the central phenyl and outer pyrimidine rings. [c] Dihedral angles between two outer pyrimidine rings.

Adjacent molecules of ligand **L1** are organized into a 1D zigzag chain by weak $\pi-\pi$ stacking interactions of 3.53−3.64 Å between the parallel neighboring aromatic rings. (see Figure S1a in the Supporting Information) This stacking is apparently different from those in **L3** and **L4** (Figure S1b and S1c in the Supporting Information). Adjacent molecules of **L3** or **L4** molecules stack on each other along the *b* direction by weak $\pi-\pi$ interaction (**L3**, 3.56−3.73 Å; **L4**, 3.53−3.64 Å). They form similar one-dimensional ribbons along the crystallographic *b* direction.[15] In addition, there

(12) (a) Rabenau, A. *Angew. Chem., Int. Ed.* **1985**, *24*, 1026. (b) Wang, R.; Zhou, Y.; Sun, Y.; Yuan, D.; Han, L.; Lou, B.; Wu, B.; Hong, M. *Cryst. Growth. Des.* **2005**, *5*, 251. (c) Feng, S.; Xu, R. *Acc. Chem. Res.* **2001**, *34*, 239. (d) Lu, J. Y. *Coord. Chem. Rev.* **2003**, *246*, 327.
(13) (a) Chesnut, D. J.; Zubieta, J. *Chem. Commun.* **1998**, 1707. (b) Chesnut, D. J.; Kusnetzow, A.; Birge, R. R.; Zubieta, J. *Inorg. Chem.* **1999**, *38*, 2663. (c) Teichert, O.; Sheldrick, W. S. *Z. Anorg. Allg. Chem.* **2000**, *626*, 2196.
(14) (a) Huang, X.-C.; Zheng, S.-L.; Zhang, J.-P.; Chen, X.-M. *Eur. J. Inorg. Chem.* **2004**, 1024. (b) Zhang, J.-P.; Lin, Y.-Y.; Huang, X.-C.; Chen, X.-M. *J. Am. Chem. Soc.* **2005**, *127*, 5495.
(15) (a) Janiak, C. *Dalton Trans.* **2000**, 3885. (b) Munakata, M.; Kuroda-Sowa, T.; Maekawa, M.; Honda, A.; Kitagawa, S. *J. Chem. Soc., Dalton Trans.* **1994**, 2771. (c) Munakata, M.; Wu, L. P.; Yamamoto, M.; Kuroda-Sowa, T.; Maekawa, M. *J. Am. Chem. Soc.* **1996**, *118*, 3117. (d) Sugimori, T.; Masuda, H.; Ohata, N.; Koiwai, K.; Odani, A.; Yamauchi, O. *Inorg. Chem.* **1997**, *36*, 576.

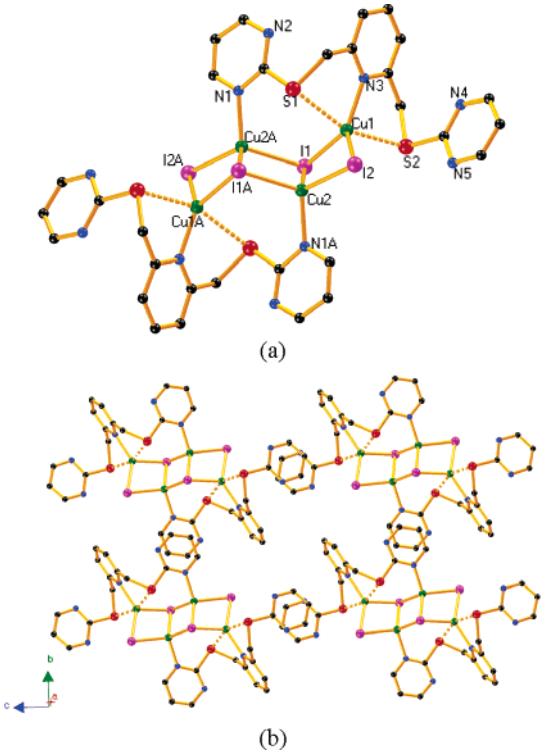

Figure 2. (a) Perspective view of **1**; (b) view of crystal packing of **1**. Symmetry code: A $-x + 2, -y + 2, -z$.

are weak C−H···S interactions (**L3**: S···H, 3.334 Å; S···H−C, 151.8°; **L4**: S···H, 3.311 Å; S···H−C, 160.8°) between adjacent $\pi-\pi$ stacking columns in **L3** and **L4**[16] that are not found in **L1,** and these weak interactions link the ribbons into a 2D undulating sheet. Generally, these weak interactions contribute to the formation and stability of the architectures. By analogy, we assume that the differences exhibited in the crystal structures by the three ligands may give rise to different metal−ligand interactions and so different products upon complexation.

Discrete Tetranuclear Complexes of $[Cu_4(L1)_2I_4]$ (1) and $[Cu_4(L1)_2Br_4]$ (2). The crystal structure of **1** consists of two **L1** ligands and a Cu_4I_4 stepped cubane, which contains two types of Cu(I) cations and two types of I anions (μ_2-I and μ_3-I) (Figure 2). One type of Cu (Cu(1)) is coordinated primarily by two I ions and one $N_{pyridine}$ atom, which define a slightly distorted trigonal planar arrangement, with the three angles ranging from 111.75(3) to 127.94(12)° and a sum of 359.7°. The 2.6200(17)−2.7380(17) Å distances between two pendant thioether sulfur atoms and the Cu(1) atom are significantly longer than those found in other four-coordinate copper(I) systems (typically ≈2.35 Å),[6] indicating only Cu···S weak interactions. Another type of Cu (Cu(2)), in the tetrahedral site, is coordinated to three I atoms and one $N_{pyrimidine}$ from another **L1** molecule. The bond angles around Cu(2), in the range 105.87(12)−113.45(3)°, are normal for a tetrahedron coordination geometry. The Cu−N distances are 2.069(4)−2.077(4) Å; the Cu−I distances are 2.5777(9)−2.7770(9) Å and are comparable to those found in reported copper iodines.[6,17]

The tetrameric Cu_4I_4 core in **1** is a distorted chairlike structure with crystallographically imposed inversion symmetry. The chairlike structure is defined by three CuICuI diamonds with each one sharing one edge with the next. Although only the central diamond is flat, the four Cu(I) atoms and four iodine atoms are precisely coplanar, thus forming two parallelograms. The Cu···Cu separation distances in the copper parallelogram show remarkable variation with short sides of 2.87771(6) Å, long sides of 3.94998(9) Å, and a short diagonal of 2.9649(15) Å, which show the $[Cu_4I_4]$ contained in **1** being more of a "flattened chair" than those reported similar substructures.[6b,17]

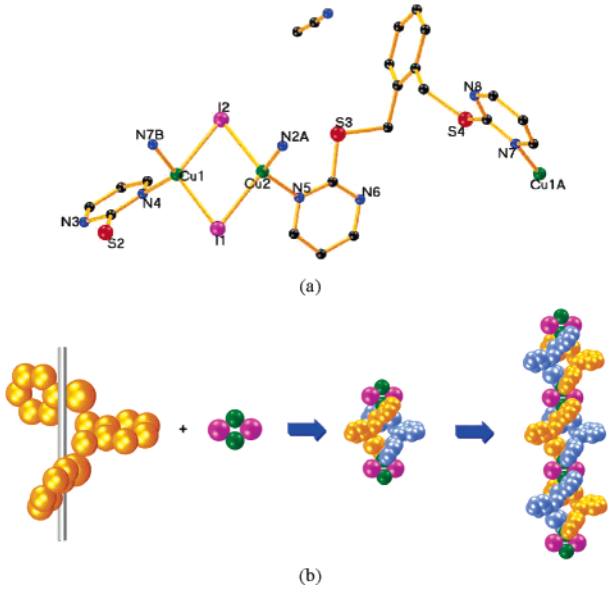

Figure 3. Complex **3**. (a) View of the coordination environment of the copper atoms, and (b) schematic representation of the formation of a 1D chain. Symmetry code: A $x, y + 1, z$; B $x, y - 1, z$.

Each **L1** ligand bridges between the two Cu(I) atoms on one side of one Cu_4I_4 structure, exhibiting a special coordination mode with the central SNS atoms chelating to Cu(1) and N atom coordinating to Cu(2A). The coordination of the terminal pyrimidine ring to the metal centers forces **L1** into a slightly shrinking conformation, increasing the dihedral angles between the central phenyl and outer pyrimidine rings from 61.5−70.3° of free ligand to 85.8−92.4°. The adjacent pyrimidine rings from different tetramers are aligned in an offset fashion; they are approximately parallel to each other with the separation of 3.2053−3.2441 Å (Figure 2b) and indicate the presence of face-to-face π-π stacking interactions.[15]

A similar reaction of CuBr with **L1** gave complex **2** $[Cu_4(\mathbf{L1})_2Br_4]$ (Figure S2 in the Supporting Information). Complexes **1** and **2** are isostructural and crystallize in the same monoclinic space group, $P2_1/n$.

1D Complexes of $[Cu_2(L2)_2I_2{\cdot}CH_3CN]_n$ (3), $[Cu(L3)I]_n$ (4), and $[Cu(L3)Br]_n$ (5). Complex **3** shows an infinite 1D chain structure and contains two crystallographically independent Cu(I) centers. As shown in Figure 3a, two Cu(I)

(16) Cargill Thompson, A. M. W.; Bardwell, D. A.; Jeffery, J. C.; Rees, L. H.; Ward, M. D. *J. Chem. Soc., Dalton Trans.* **1997**, 721.
(17) (a) Rath, N. P.; Holt, E. M.; Tanimura, K *J. Chem. Soc., Dalton Trans.* **1986**, 2303. (b) Kuhn, N.; Fawzi, R.; Grathwohl, M.; Kotowski, H.; Steimann, M. *Z. Anorg. Allg. Chem.* **1998**, *624*, 1937.

ions display similar distorted tetrahedral coordination geometry comprised of two bridging iodine ions and two N donors from different pyrimidine rings of two distinct ligands, with the angles varying from 100.59(7) to 120.38(9)°. The Cu−I and Cu−N bond lengths are in the range of 2.6166(4)−2.7125(5) and 2.044(2)−2.072(2) Å, respectively, which are normal ranges.[6,17] Two μ_2-iodine ions are bound to two adjacent, different Cu(I) centers, forming a CuI_2Cu rhomboid dimer in which the Cu(I) centers are separated by a distance of 3.0262(6) Å. Two bis-monodentate **L2** ligands wrap around the Cu−Cu axis of two adjacent CuI_2Cu rhomboid dimers, with a separation of 9.7664(2) Å, giving rise to a $[Cu_2\mathbf{L2}_2]^{2+}$ double-helical subunit. The subunits further extend along the crystallographic *b* axis by μ_2-I atoms bridging the $[Cu_2(\mathbf{L2})_2]^{2+}$ double-helical dinuclear subunits to form an infinite 1D chain (Figure 3b). In other words, $[Cu_2(\mathbf{L2})_2I_2]_n$ can be considered as being a double-stranded helix generated by the intertwining of two single-stranded helical chains and separated by μ_2-iodine ions. All Cu atoms are almost in line with a Cu1−Cu2−Cu1A angle of 177.6° and are positioned at the central helical axis. Many discrete helical structures[18] and infinite helical coordination polymers[19] have been synthesized over the past decade. However, to the best of our knowledge, such a 1D chain formed by discrete double helicates linked via bridging iodine ions has not been reported to date. Except for C−H···S weak interactions (S···H, 3.171Å; S···H−C, 169.0°) found between adjacent chains,[16] there are no obvious intermolecular $\pi-\pi$ interactions between aryl rings. In addition, acetonitrile solvent molecules are filled in the interspace of adjacent chains and show no interactions with other molecules.

The reaction of CuI with **L3** leads to the formation of a one-dimensional double-stranded helical complex $[Cu(\mathbf{L3})I]_n$ **4**, which contains a CuI_2Cu connector different from that in **3**. As shown in Figure 4a, the Cu(I) adopts a distorted tetrahedron arrangement with a coordination sphere provided by two μ_2-iodine ions and two $N_{pyrimdine}$ donors from different **L3** ligands. The bond angles around Cu(1), in the range 93.34(8)−137.02(11)°, form a more distorted geometry than that in **3**, and the Cu−I bond distances ranging from 2.6865(6) to 2.8424(6) Å are significantly longer than those in **3** and other tetrahedral Cu(I) coordination systems.[6,17] Each pair of adjacent Cu(I) atoms is bridged by an **L3** ligand to afford a single chiral helical chain running along the *c* direction with a short pitch of 8.973 Å. Two adjacent single-stranded helical chains with the same handedness are further joined together through a middle CuI_2Cu connector to form a double-stranded helix (Figure 4b). Such double-stranded helical chains formed by halogen-ion bridging have not been

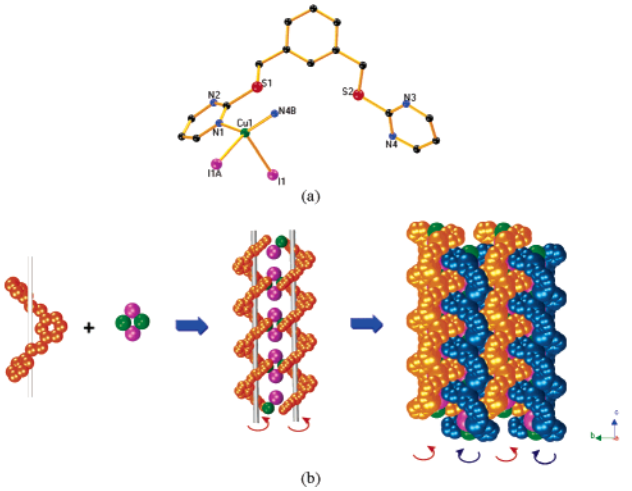

Figure 4. Complex **4**. (a) View of the coordination environment of the copper atoms, and (b) schematic representation of the formation of the 1D chain. Symmetry codes: A $-x+2, y, -z+{}^5/_2$; B $x, y, z+1$.

documented. It is noteworthy that although the double-stranded helical chain is a chiral one, with either left- or right-handedness, the whole structure is achiral with centrosymmetric space group *C*2/*c*, which originates from the alternate stacking of helical chains with opposite chirality. The **L3** pyrimidine rings at each side of the helix are arranged in a parallel fashion with an interring distance of 6.5766−6.7192 Å, resulting in a structure suitable for forming aromatic intercalation.[19d] So adjacent chiral helices are racemically packed through intercalation of the lateral pyrimidine rings in a zipperlike, offset fashion (face-to-face distances of 3.2769−3.3866 Å) into two-dimensional layers parallel to the *bc* plane (Figure 4b). Similar zipperlike intercalations have been reported previously in some three-dimensional coordination architectures constructed by two-dimensional layers.[20] These 2D layers are further extended into the final three-dimensional (3D) networks through strong aromatic $\pi-\pi$ interactions between phenyl rings from adjacent layers, with a center-to-center distance of about 3.809 Å.

To examine the role of halide atoms in the formation of double-stranded helical chains, we used CuBr instead of CuI to produce complex **5**. Single-crystal X-ray diffraction analysis has proved that complexes **4** and **5** are isomorphous (see Figures S3 in the Supporting Information).

2D complexes of $[Cu(L3)CN]_n$ (6), $[Cu(L4)CN]_n$ (7), $[Cu_2(L4)I_2]_n$ (8), and $[Cu_2(L4)(SCN)_2]_n$ (9). As shown in Figures 5 and 6, complexes **6** and **7** show a similar 2D undulating sheet formed by ligand molecules bridging $[Cu(CN)]_n$ chains. For the crystals of **6**, with block morphology, the asymmetric unit consists of a copper site with a site occupancy of 0.5, one C/N site of cyanide and half **L3** molecules. This is different from the basic unit of **7**, which contains a Cu(I) ion, a complete ligand (**L4**), and one μ-CN^- anion. The Cu(1) center in **6** is coordinated to two C/N atoms from cyanide groups in a nonlinear fashion, and C/N(1)−

(18) (a) Guo, D.; He, C.; Duan, C. Y.; Qian, C. Q.; Meng, Q. J. *New J. Chem.* **2002**, *26*, 796. (b) Lehn, J.-M.; Rigault, A. *Angew Chem., Int. Ed.* **1988**, *27*, 1095. (c) Hannon, M. J.; Painting, C. L.; Alcock, N. W. *Chem. Commun.* **1999**, 2023.

(19) (a) Huang, X.-C.; Zhang, J.-P.; Lin, Y.-Y.; Chen, X.-M. *Chem. Commun.* **2005**, 2232. (b) Mamula, O.; Zelewsky, A. V.; Bark, T.; Bernardinelli, G. *Angew. Chem., Int. Ed.* **1999**, *38*, 2945. (c) Tabellion, F. M.; Seidel, S. R.; Arif, A. M.; Stang, P. J. *Angew. Chem., Int. Ed.* **2001**, *40*, 1529. (d) Chen, X.-M.; Liu, G.-F. *Chem.—Eur. J.* **2002**, *8*, 4811. (e) Cui, Y.; Lee, S. J.; Lin, W. *J. Am. Chem. Soc.* **2003**, *125*, 6014.

(20) (a) Tong, M.-L.; Chen, H.-J.; Chen, X.-M. *Inorg. Chem.* **2000**, *39*, 2235. (b) Zheng, S.-L.; Tong, M.-L.; Fu, R.-W.; Chen, X.-M.; Ng, S.-W. *Inorg. Chem.* **2001**, *40*, 3562.

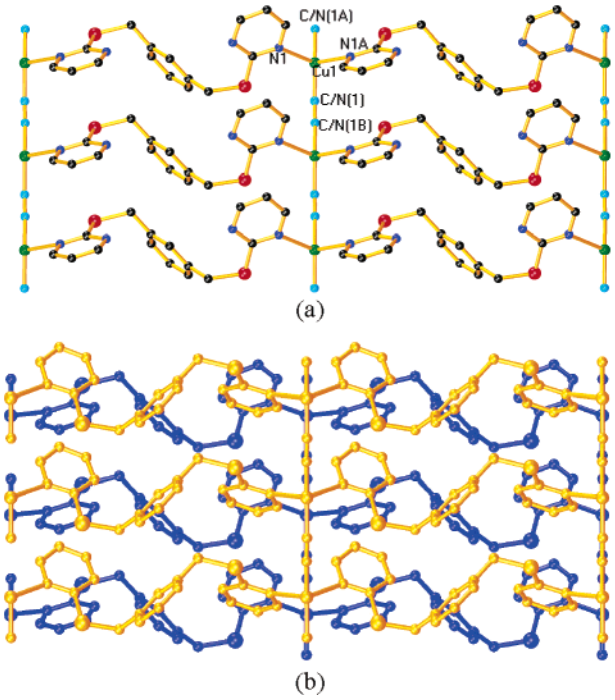

Figure 5. (a) View of the 2D network in **6** from the *c* axis, and (b) packing diagram for **6**. Symmetry codes: A $-x+1, -y, z$; B $-x+1, -y+1, z$.

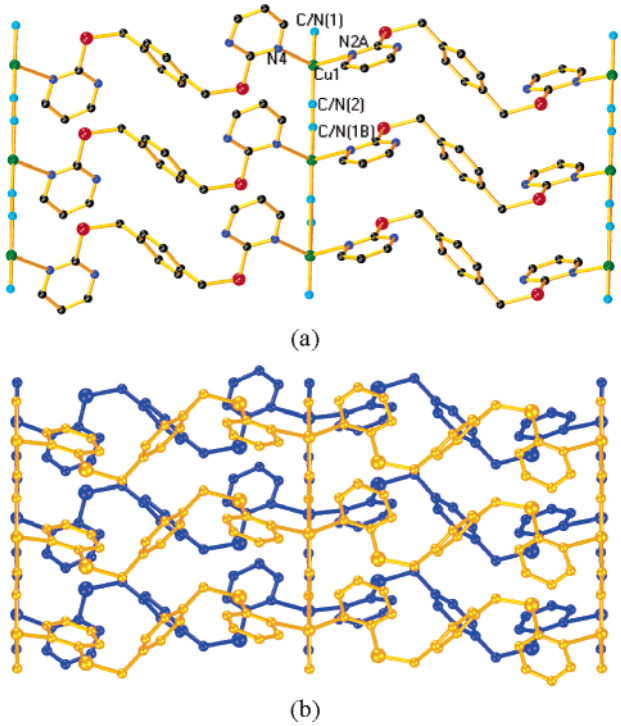

Figure 6. (a) View from the *a* axis showing the 2D network of **7**, and (b) packing diagram for **7**. Symmetry codes: A $^1/_2 - x, y, -^1/_2 + z$; B $x, y-1, z$.

C/N(1B) bond lengths of 1.134(14) Å and Cu−C/N distances of 1.885(7) Å are comparable to those found in reported copper cyanide.[21] Besides these strong bonds, there are also weak coordination interactions between the copper and two adjacent thioether N atoms with the same distance of 2.431(6) Å, which was above the range of 1.96−2.14 Å found for the Cu(I)−N bond distances of such compounds[7b,22] but within sum of the van der Waals radius of 2.95 Å. If all these interactions are taken into account, the Cu(1) atom has a very distorted 2+1+1 tetrahedral environment, with the bond angles around Cu(1) varying substantially from 91.9(3) to 155.2(4)°. In **7**, the Cu(I) center has coordination environment similar to that of **6** and is bound by two C/N atoms from cyanide groups and two pyrimidine nitrogen atoms from two distinct **L4** ligands. The mean values of the Cu−C/N, Cu−$N_{pyrimdine}$, and C/N−C/N distances (1.880(5), 2.427(5), and 1.152(6) Å, respectively) and the distorted tetrahedral coordination geometry (bond angles in the 93.2−154.96(16)° range) in **7** can compare with those of **6**. The extended infinite zigzag $[Cu-CN]_n$ chains running along the *b* axis, with a Cu···Cu separation between adjacent chains of 14.0560(4) and 14.14(1) Å in **6** and **7**, respectively, are further connected by parallel ligand molecules via Cu−$N_{pyrimdine}$ coordination interactions, affording a two-dimensional pucker layer. The 2D sheet in **7** expresses a stronger corrugated figure than that in **6**. The aromatic face-to-face distance of 3.5619−3.886 Å between the neighboring ligand reveals weak $\pi-\pi$ interactions.[15] Each sheet reverses from its neighbors and lies on top of the others along the *c* or *a* axis for complex **6** or **7**, respectively. This is consistent with different orthorhombic space groups *Pnc*2 and *Pca*2_1, which show an ABAB packing mode (Figure 5b and 6b).

Unlike that in other Cu(I) halide complexes discussed above, the difference in ligand spacers in **L3** and **L4** in **6** and **7**, respectively, causes only subtle geometrical differences in their CuCN complexes and does not greatly influence the whole structure topology. We suppose that the stability of the [Cu−CN] zigzag chain formed by μ-CN^- coordinated to Cu(I) seems to be a determining factor affecting the coordination frameworks of **6** and **7**, which overcome the influence of different ligands (**L3** and **L4**) on the metal−ligand frameworks.

The crystal structure of $[Cu_2(\mathbf{L4})I_2]_n$ (**8**) contains a very simple asymmetric unit, but the resulting extended structure is a robust lamellar solid (Figure 7). Each tetrahedral Cu(I) ions is coordinated to three μ_3-I ligands, which generates a 1D $[CuI]_n$ staircase along the crystallographic *a* axis, leaving one site available for the fourth bond with ligand **L4** through the pyrimidine nitrogen atom (Cu(1)−N(1), 2.017(3) Å). The geometry of Cu(1) is quite distorted, with I−Cu−I angles ranging from 96.92(10) to 138.75(9)° and N−Cu−I bond angles in the range of 92.51(2)−112.99(2)°. The Cu(1)−I(1B) distance of 3.0338(8) Å is remarkably longer than the other two similar coordination bonds (Cu(1)−I(1), 2.5601(7) Å; Cu(1)−I(1A), 2.6939(7) Å), as well as those found in reported copper iodides.[6,17] Therefore, the long Cu−I bonds can be considered as being spacers bridging two zigzag single chains and forming a $[CuI]_n$ staircase structure. The distances (3.327−3.883 Å) between diagonal copper atoms are too

(21) (a) Zhang, X.-M.; Fang, R.-Q. *Inorg. Chem.* **2005**, *44*, 3955. (b) Hanika-Heidl, H.; Etaiw, S. E. H.; Ibrahim, M. S.; El-din, A. S. B.; Fischer, R. D. *J. Organomet. Chem.* **2003**, *684*, 329. (c) Stocker, F. B.; Staeva, T. P.; Rienstra, C. M.; Britton, D. *Inorg. Chem.* **1999**, *38*, 984. (d) Chesnut, D. J.; Plewak, D.; Zubieta, J. *J. Chem. Soc., Dalton Trans.* **2001**, 2567.

(22) (a) Wang, R.-H.; Hong, M.-C.; Su, W.-P.; Liang, Y.-C.; Cao, R.; Zhao, Y.-J.; Weng, J.-B. *Bull. Chem. Soc. Jpn.* **2002**, *75*, 725. (b) Simmons, C. J.; Lundeen, M.; Seff, K. *Inorg. Chem.* **1979**, *18*, 3444.

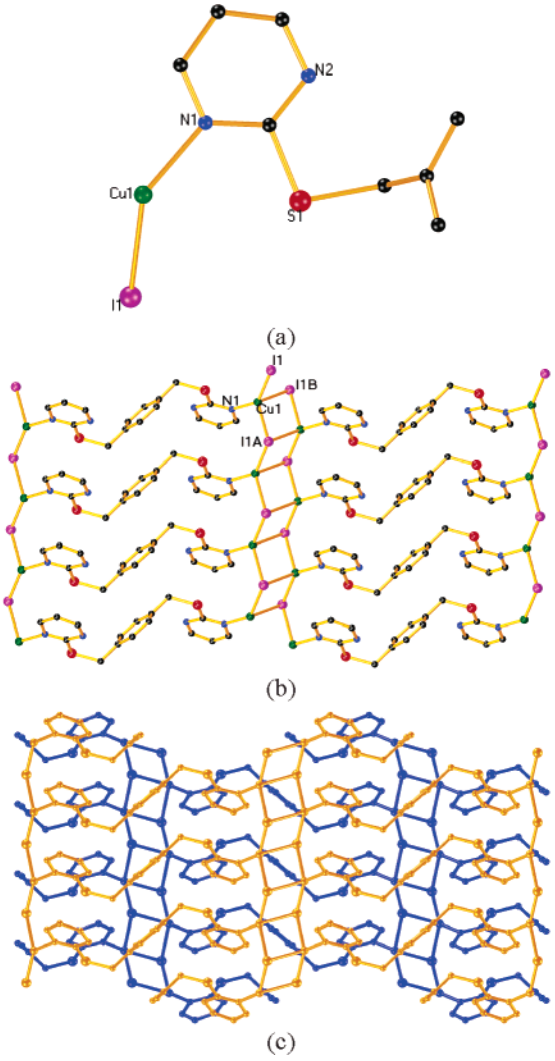

Figure 7. (a) Asymmetric unit of **8**; (b) perspective view of the 2D network of **8**; and (c) stacking pattern for **8**. Symmetry codes: A $x + 1$, y, z; B $-x + 1$, $-y + 2$, $-z + 1$.

long to consider Cu···Cu interactions. The bis-monodentate ligand acts as a bridge between $[CuI]_n$ staircases and serve to propagate the 1D polymeric chains into infinite 2D layers. The interplanar spacing of 3.5142 Å indicates $\pi-\pi$ interactions between adjacent **L4** molecules.[15] Each sheet is reversed and offset from its neighbors, expressing an ABAB stacking pattern (Figure 7c). No remarkable short contacts or noteworthy aryl−aryl interactions are found between adjacent sheets.

X-ray structural analysis of **9** reveals a two-dimensional sheet structure (Figure 8) containing two different Cu(I) centers. Tetrahedral Cu(1) is coordinated by two μ_2-S atoms from two bridging thiocyanate ligands and by two N atoms from different bis-monodentate **L4** molecules. The other ends of the two μ_2-S atoms are bound to the second Cu(I) center, Cu(2), forming a CuS_2Cu cyclic unit that serves as the polymeric link for the system. The Cu(I) centers are separated by a relatively long distance of 3.019(1) Å, which is comparable to that of 3.0262(6) Å in **3** and shorter than those of 3.4560(1) Å in **4** and 3.327−3.883 Å in **8** but longer than the sum of their van der Waals radii (2.8 Å), indicating no Cu−Cu weak interaction. The remaining two sites of Cu(2)

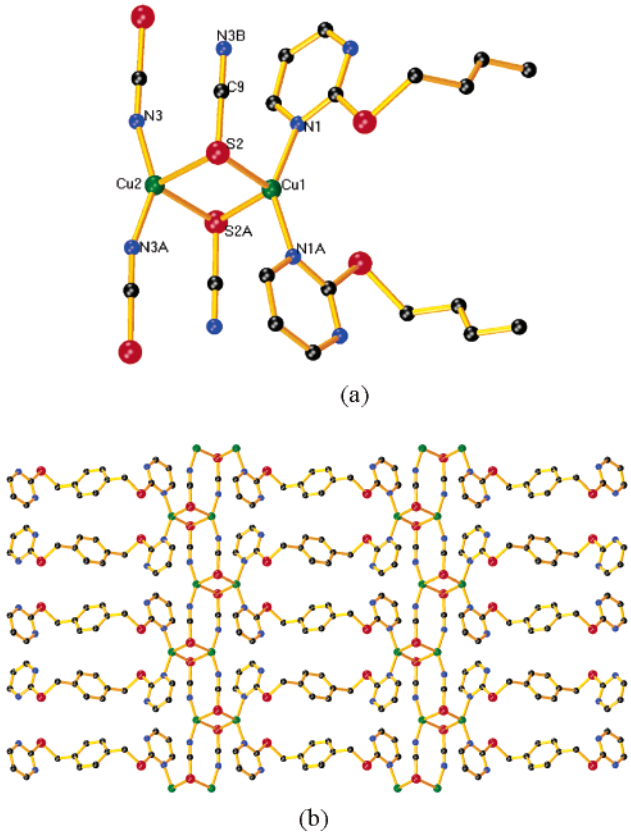

Figure 8. Complex **9**. (a) Views of the copper(I) coordination environment, and (b) perspective view of the 2D network. Symmetry codes: A $-x + 2$, y, $-z + 5/2$; B $-x + 2$, $-y$, $-z + 2$.

adopt a distorted tetrahedral geometry and are occupied by two N atoms from another two bridging thiocyanate ligands. The geometry of all Cu(I) centers is quite distorted, with N−Cu−N angles of 144.47(12)−147.71(15)°, S−Cu−S angles of 103.36(4)−110.40(4)°, and N−Cu−S angles ranging from 98.80(6) to 101.26(6)°. The thiocyanate groups function as tridentate μ-S,S,N bridges connecting three different metal centers, resulting in a $[CuSCN]_n$ displaced stair polymer extended along the *c* axis of the unit cell. This is a new framework for the CuSCN system, and similar examples of this displaced stair motif have been found only for $[CuX]_n$ (X = Br, I).[23] However, a number of comparable stair polymer arrangements have been observed before for $[Cu_2(SCN)_2(bpe)]_n$ (bpe = *trans*-1,2-bis(4-pyridyl)ethane), $[Cu(SCN)(dpt)]_n$ (dpt = 2,4-bis(4-pyridyl)-1,3,5-triazine), and $[Cu(SCN)(2\text{-Mepy})]_n$ (2-Mepy = 2-methylpyridine)[24] (see comparison between $[Cu(SCN)]_n$ displaced stair polymer and stair polymer in Figure S4 in the Supporting Information). The generation of a displaced stair instead of a stair polymer indicates that the steric constraint on the ligands force the stair to deviate.

(23) (a) Massaux, M.; Ducreux, G.; Chevalier, R.; Bihan, M.-T. L. *Acta Crystallogr., Sect. B* **1978**, *34*, 1863. (b) Fisher, P. J.; Taylor, N. F.; Harding, M. M. *J. Chem. Soc.* **1960**, 2303.

(24) (a) Barnett, S. A.; Blake, A. J.; Champness, N. R.; Wilson, C. *Chem. Commun.* **2002**, 1640. (b) Blake, A. J.; Brooks, N. R.; Champness, N. R.; Crew, M.; Hanton, L. R.; Hubberstey, P.; Parsons, S.; Schröder, M. *J. Chem. Soc., Dalton Trans.* **1999**, 2813. (c) Healy, P. C.; Pakawatchai, C.; Papasergio, R. I.; Patrick, V. A.; White, A. H. *Inorg. Chem.* **1984**, *23*, 3769.

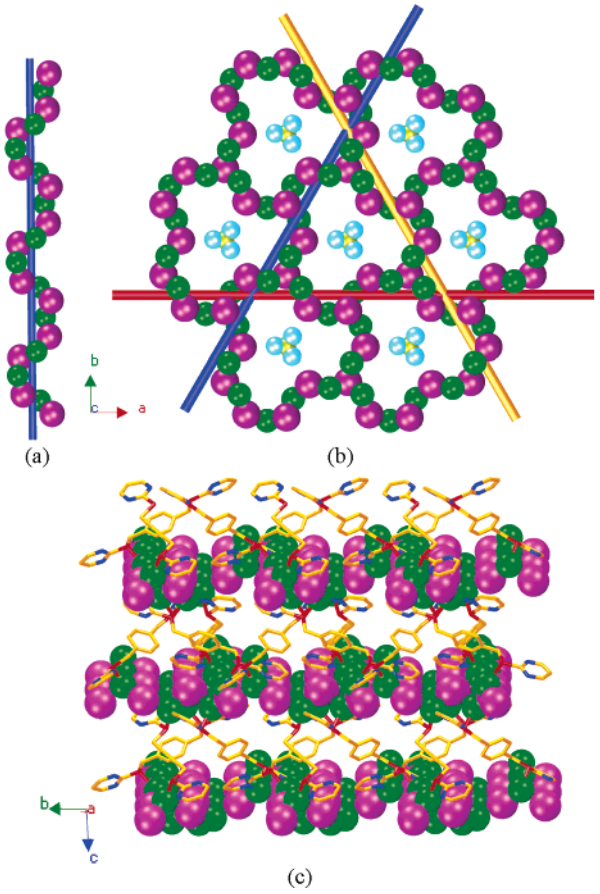

Figure 9. Complex **10**. (a) Single $[CuI]_n$ helix; (b) $[(Cu_6I_5)^+]_n$ layer constructed by intersecting $[CuI]_n$ helices extended along the [100], [010], and [110] directions. (c) 3D view showing the alternate inorganic−organic stacking (green, purple, yellow, and pale-blue spheres represent Cu, I, B, and F atoms, respectively).

In parallel running, infinite $[CuSCN]_n$ stairs are tied together by bridging bis-bidentate **L4** ligands to form 2D sheets. Adjacent sheets pack closely along the *a* axis with a staggered arrangement so that the $[(CuSCN)_2]_n$ displaced stair polymers sit perpendicularly above **L4** ligands in adjacent sheets. There are face-to-face stacking interactions between the intersheet parallel pyrimidine rings, with a centroid−centroid separation of 3.607 Å.[15]

3D complex of $\{[Cu_6I_5(L4)_3](BF_4)\cdot H_2O\}_n$ (10). The 3D structure of **10** is constructed by a 2D inorganic $[(Cu_6I_5)^+]_n$ layer connected by ligand **L4** through nitrogen and sulfur atoms. Interestingly, the $[(Cu_6I_5)^+]_n$ layer is built by intersecting 1D $[CuI]_n$ right-handed helices (Figure 9a, b) in three different directions, effectively forming an undulating pseudohexagonal net. Because the helical network in the (6,3)-topology net is right-handed, the net as a whole in this case is known as being right-handed. Alternate inorganic $[(Cu_6I_5)^+]_n$ lamellae and organic thioether ligand **L4** layers, expressed as an ABAB repeating pattern, extend to form a 3D network (Figure 9c). Disordered water molecules and BF_4^- anions fill in the network. A discussion of the structure detail was given in our recent communication.[8]

Photoluminescence Properties. Complexes **1**−**10** are stable in air. Complexes **1**−**3** do not exhibit detectable emission, whereas **4**−**10** show strong photoluminescence upon irradiation of ultraviolet light in the solid state. Unfortunately, no photoluminescence measurement in solution can be carried out, because **4**−**10** cannot be dissolved in common organic solvents. The emission spectra of the seven Cu(I) complexes have been recorded in the solid state at room temperature, and the spectral data are summarized in Table 6. In comparison with the photoluminescence properties of reported complexes of cuprous halides and heterocyclic ligands, we tentatively assigned the emission of the Cu(I) complexes as being a metal center (MC) d−s state or a metal-to-ligand charge-transfer (MLCT) state for their broad and structureless emission spectra, as free ligands **L1**−**L4** do not show photoluminescence.[7b,14b,25] The emission peaks for **6** and **7** are quite similar, with only 2 nm difference in the yellow range (Figure 10), which is in agreement with their similar extended architectures. Compared to **6** and **7**, complexes **4**, **5**, and **8**−**10** have higher-energy transitions, which may be ascribed to the different coordination bonds as shown Table 6. Because the energies of a frontier molecular orbit would certainly be dependent on the extent of mixing due to metal−ligand covalent interaction, the large red shift of the emission maximum of **6** and **7** may be ascribed to a weak coordination interaction of the long Cu−N and Cu−Cu distances.

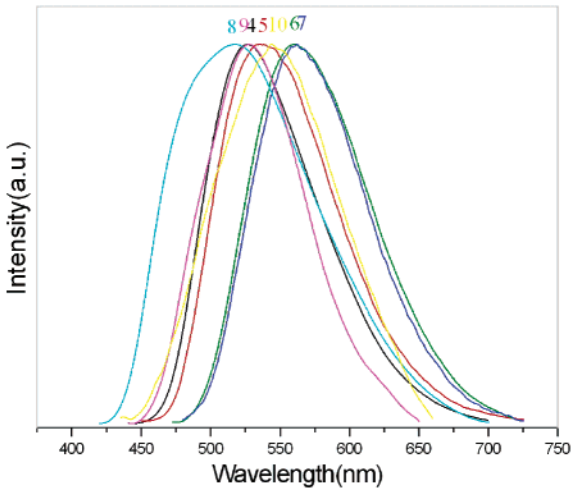

Figure 10. Emission spectra of the Cu(I) complexes in the solid state at room temperature.

Table 6. Emission Data of the Cu(I) Complexes

complex	Cu−Cu (Å)	Cu−N (**L**) (Å)	λ_{ex} (nm)	λ_{em} (nm)
4	3.4560(1)	2.013(3)	395, 442	525
5	3.4343(1)	1.9972(17)	390	535
6	4.8159(1)	2.431(6)	393	560
7	4.820(4)	2.333(7)−2.521(2)	393	562
8	3.327−3.883	2.017(3)	393, 437	517
9	3.019(2)	2.031(2)	338, 393	525
10	3.674−3.754	2.030(7)−2.049(6)	345, 385	535

Conclusion

The self-assembly of flexible pyrimidine-based thioether ligands **L1**−**L4** and copper(I) halides or pseudo-halides

(25) (a) Araki, H.; Tsuge, K.; Sasaki, Y.; Ishizaka, S.; Kitamura, N. *Inorg. Chem.* **2005**, *44*, 9667. (b) Ford, P. C.; Cariati, E.; Bourassa, J. *Chem. Rev.* **1999**, *99*, 3625.

Chart 2. Schematic Illustration of Complexes **3**−**10**[a]

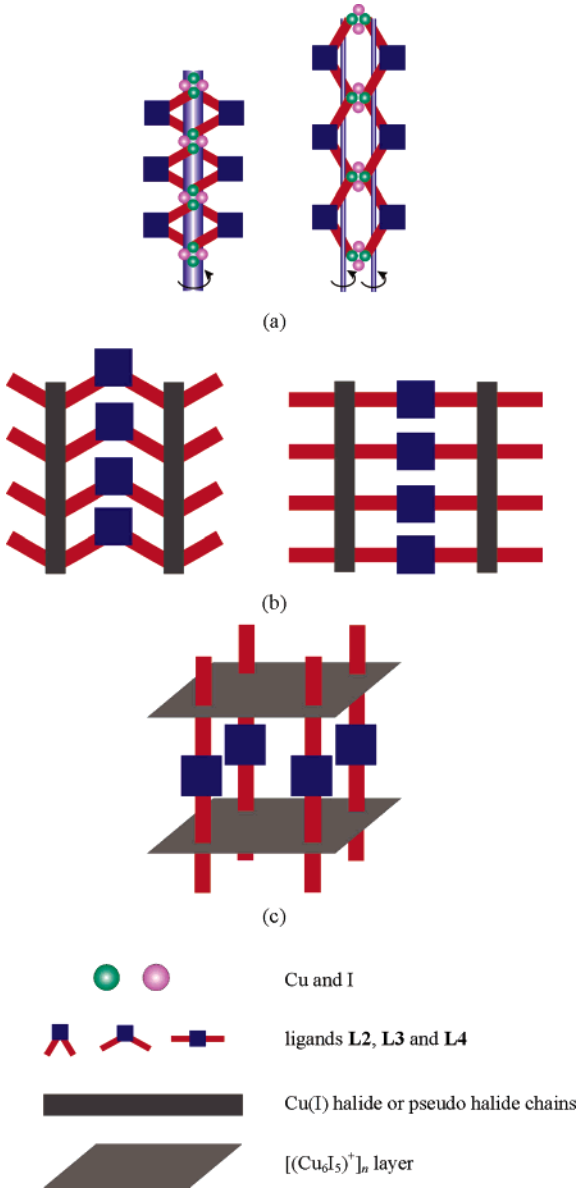

forms a series of complexes from discrete molecules to extended architectures with increasing dimensionality, as schematically shown in Chart 2. The structural differences of oligomers of **1** and **2** and polymers of **4** and **5** can be explained by the one noncoordinated C atom in central benzene of **L3** being replaced by a strong donor N atom of **L1**, which resulted in the SNS chelating coordination moiety in **1** and **2**. Excerpt for in **10**, there are no significant Cu−S interactions found in **1**−**9,** which may be due to the geometrical effects being more preferential than electronic effects in these complexes; this also leads to the soft Cu(I) center tending to coordinate to N donors rather than S donors. Three CuI complexes of **L2**−**L4** provide considerable evidence to support the contention that ligand geometry influences the formation of metal−ligand frameworks.

To be worthy of comparison, iodide adducts **3**, **4**, and **8** bear significant difference. This may be attributed to the differences in the bite angles of the three corresponding ligands, with the disposition of their lone pairs varying from acute (bridging angle 60°, as in **L2**) through obtuse (bridging angle 120°, as in **L3**) to linear (bridging angle 180°, as in **L4**), though this kind of geometry effect of flexible ligands is considerably weakened when comparing rigid ligands, because of the free rotation of the S−CH_2 arm.

On the other hand, the changes in counterion also cause certain geometrical differences, as is the case in **7**−**9**. Three different 1D copper halide or pseudo-halide frameworks, zigzag chain, stair, displaced stair, are found, respectively, in the three complexes and are further connected through the bridging flexible ligand to construct a two-dimensional layer network. The structural variety of these 1D frameworks may be attributed to the differences in coordination properties of the incorporated counteranions μ_3-I^-, μ-CN^-, and 1,1,3-μ_3−SCN^-. It must be mentioned that although it uses the same ligand, the 3D polymer **10** is a surprising contrast to the two-dimensional networks in **7**−**9**.[8] Both types of iodide anion (μ_3-I and μ_2-I) are incorporated into the $[Cu_6I_5]^+$ layer in **10,** as well as the capsulated BF^- anion, which may act as a template of the coordination polymer and effectively balance the charge of $[Cu_6I_5]^+$ layer. This further demonstrates the significant role of the anion in the preparation and structures.

The set of structures exemplifies the influence of various factors such as ligand geometry, the nature of the anions, and $\pi-\pi$ stacking on the self-assembly of diverse coordination aggregates with Cu(I**)** salts. This work offers the possibility to control the formation of such network structures by varying those factors.

Acknowledgment. The authors gratefully acknowledge the financial support provided by the National Natural Science Foundation of China (20571050 and 20271031) and the Natural Science Foundation of Guangdong Province of China (021240).

Supporting Information Available: Crystallographic files in cif format and supplementary illustration for the structures. This material is available free of charge via the Internet at http://pubs.acs.org.

IC060074X